Supplementary Information for:

Decreasing intensity of monsoon low-frequency intraseasonal variability over India

Nirupam Karmakar, Arindam Chakraborty,

& Ravi S. Nanjundiah

Supplementary Information README

1 Multichannel Singular Spectrum Analysis (MSSA):

To extract oscillatory components present in the monsoon variability we applied MSSA to the intraseasonally filtered May–October data (N=184 days long) each year. Each year is treated separately because we do not want any discontinuity in the rainfall time series. Additionally, since the characteristics of the intraseasonal variability vary on a year-to-year basis, it makes sense to examine each year individually. Here, the embedding window length (M) is taken as 60 days, which satisfies the criteria to choose M ($M \leq N/3$), as described in [1]. Switching M to 50 does not alter the conclusions. $N'=N-M+1$ (=125) can be treated as a complementary window, and an N'xN' matrix (reduced lag-covariance matrix) can be formed to obtain ST-PCs and ST-EOFs [2, 3]. The (reduced) ST-PCs are the eigenvectors of the reduced covariance matrix. Since, the non-zero eigenvalues of both LMxLM and N'xN' matrices are same, we used computationally more efficient reduced covariance matrix approach. These ST-EOFs and ST-PCs describe the "skeleton" of the dynamical system and we can reconstruct trends, oscillatory modes, and irregular "noise" using linear combination of these components. Reconstruction of the part of the time series associated with a single mode (or several) is done by convolving the corresponding ST-PC with ST-EOF (and combining them). Essentially, these reconstructed components (RCs) represents a narrowband of the full frequency spectrum. Usually, an oscillation is identifiable if eigenvalues associated with two RCs are nearly equal and corresponding eigenvectors represent almost equal dominant frequency with phase quadrature. The sum of these individual pair of RCs represents the oscillation. A statistical test is performed by comparing the variance captured by an ST-EOF with that present for the same in a large ensemble (1000) of red-noise surrogates [2, 4]. This test is done to avoid any random fluctuation being treated as an oscillation. Here we note that the channels feed into MSSA algorithm are needed to be uncorrelated at lag-0, which is a necessary condition for testing the significance of the ST-EOFs [4]. So we perform a standard principal component analysis (PCA) and carry the PCs (which are orthogonal by definition) into MSSA without losing any information.

The amplitude and the phase angle of the oscillation can be determined using the first principal component (PC) of a particular reconstructed oscil-

latory component [5]. Essentially, phase angle ($\theta(t)$) lies in (0,2π) and it is divided into eight equally spaced intervals such that $(m-1)\pi/4 \leq \theta(t) < m\pi/4$ with m=1,...,8. Regardless of the amplitude, averaging the reconstruction over all occurrences in a particular phase gives phase composite.

It has been shown that classical MSSA suffers from a degeneracy problem [6]. The eigenvectors cannot distinguish between uncoupled, distinct systems, producing a mixture in different modes and as number of channels increases, this effect intensifies. Also, all PCA methods try to maximize variance captured by successive eigenvectors and create artificial variance compression. To overcome these effects and improve physical interpretability, a modified varimax rotation of the ST-EOFs is done [6]. Here, 20 eigenvectors are rotated to make sure that at least the significant eigenvectors are included.

2 Determining the phases of ISO: Active/break phases

In order to determine the phase of an ISO cycle at a particular gridpoint, we use the following equation:

$$\gamma(t) = Arg(Y'(t) + iY(t)) \tag{1}$$

where, t denotes time, $Y(t)$ is the 184 day long (May–October) ISO (LF-ISO or HF-ISO) time series at any point and ($'$) indicates the time-derivative. $Arg(z)$ represents the principal value of the phase of a complex number z=$x + iy$. $\gamma(t)$ is calculated at every gridpoint each year and lies between -π and π. Active (positive), break (negative) and transition phases of ISO are defined based on the values of $\gamma(t)$. For example, in figure S3, $\gamma(t)$ is calculated for LF-ISO at a gridpoint in central India for May–October, 1951. The active, break and transition phases are defined in the following way: If for a value of t, $\gamma(t)$ lies within $\pi/6$ and $5\pi/6$, ISO is in active (positive) phase, and if $\gamma(t)$ lies within -$5\pi/6$ and -$\pi/6$, ISO is in break (negative) phase. The rest of the values of $\gamma(t)$ determines the transition phase.

3 Determining trends and significance levels

We adopted Mann-Kendall non-parametric test to identify the significant trends [7]. No assumption of normality is required for this test, but a check for serial correlation is done a priori using Durbin-Watson statistic to make sure there exists none. Associated slopes are estimated using the median of all pairwise slopes in the data set (Theil-Sen estimator) [7].

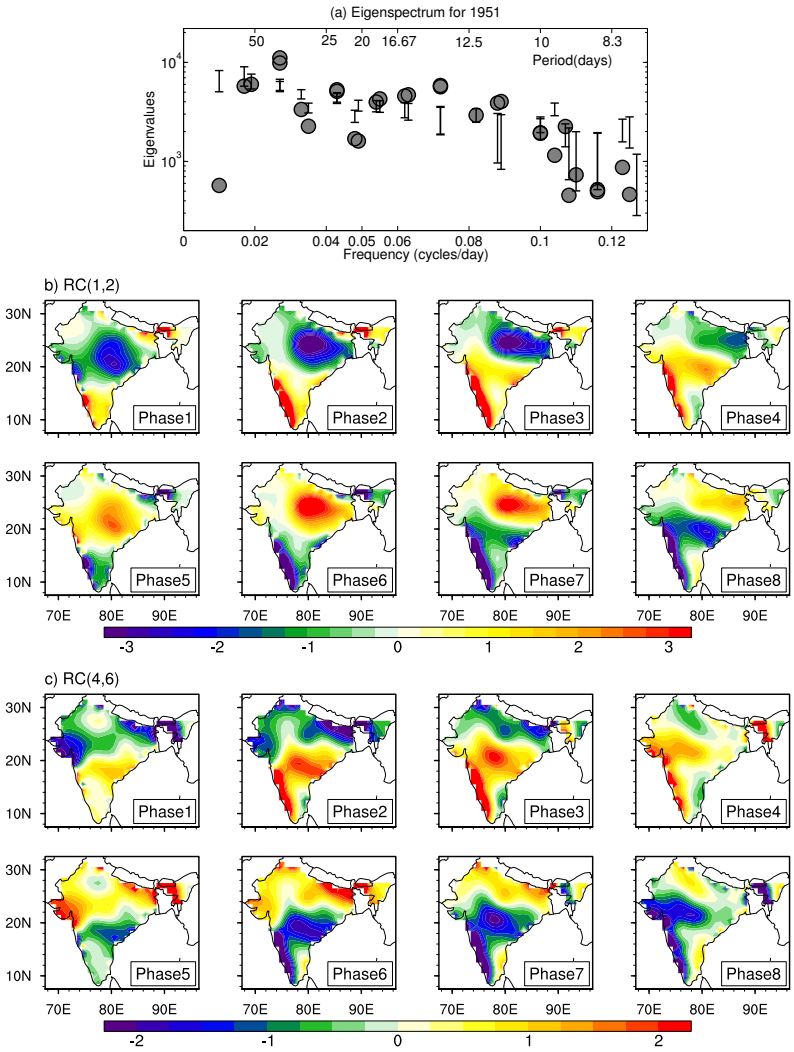

Figure S1: **(a)** Eigenvalues from MSSA for 1951 May–October rainfall over India against the dominant frequency associated with their corresponding eigenvectors from MSSA given with statistical significance level (zoomed into the region of interest). Error bars represent the 2.5% and 97.5% quantile from an ensemble of 1000 surrogate data. Eigenmodes which lie above the corresponding errorbars are considered as significant. For example, eigenmodes 1 and 2 with periodicities almost 37 days and eigenmodes 4 and 6 having periodicities approximately 14 days are considered as significant. Significant modes with time-periods within 10-20 and 20-60 are considered as HF-ISO and LF-ISO modes, respectively. Phase composite of **(b)** $RC(1,2)$ which has a periodicity of about 37 days showing north-eastward propagation and **(c)** $RC(4,6)$ which has a periodicity of almost 14 days, showing north-westward propagation during May–October, 1951. Units are in mm/day. $RC(i,j)$ indicates reconstructed components associated with eigenmodes i and j.

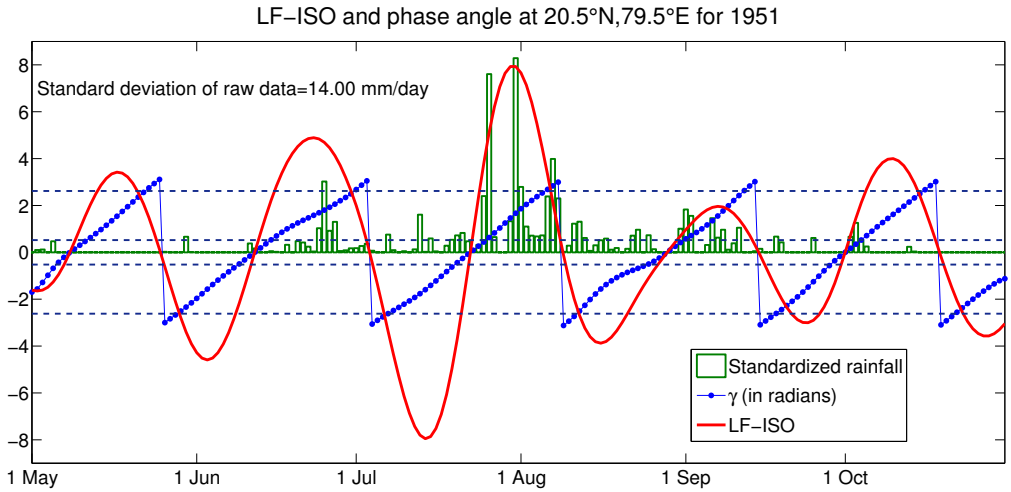

Figure S2: Defining the phases of LF-ISO at a particular location ($20.5°N$, $79.5°E$) in 1951. Red curve indicates the LF-ISO and green boxes are the standardized rainfall at that location. Units are in mm/day. The phase angle (γ) is shown by blue dots (in radians). Dotted straight lines indicate -$5\pi/6$, -$\pi/6$, $\pi/6$, and $5\pi/6$ lines. If for a value of t, $\gamma(t)$ lies within $\pi/6$ and $5\pi/6$, LF-ISO is in positive (active) phase, and if $\gamma(t)$ lies within -$5\pi/6$ and -$\pi/6$, LF-ISO is in negative (break) phase. The rest of the values of $\gamma(t)$ determines the transition phase. Values of $\gamma(t)$ between -$\pi/6$ and $\pi/6$ gives negative-to-positive and $\gamma(t)$ between $5\pi/6$ and π, and -π and -$5\pi/6$ gives positive-to-negative transition phases.

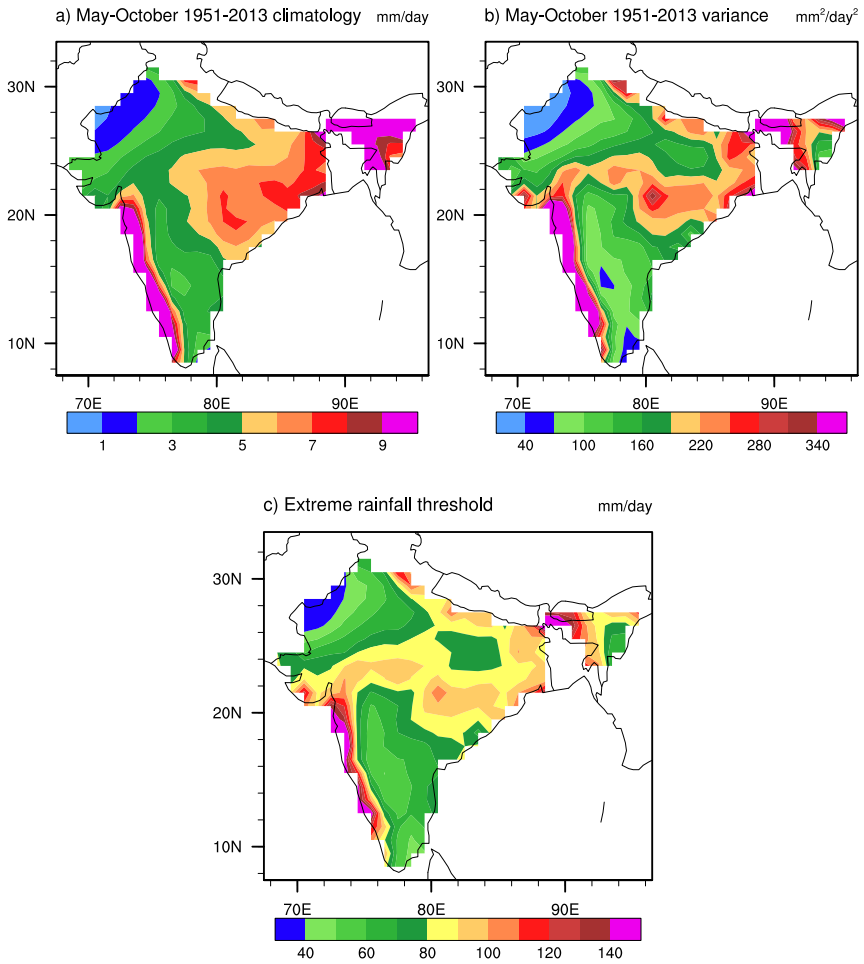

Figure S3: **(a)** May–October climatology for 1951–2013 period. Unit is in mm/day. **(b)** May–October variance of daily rainfall for 1951–2013. Unit is in mm^2/day^2. **(c)** Spatial distribution of extreme rainfall threshold over India set as the 99.5^{th} percentile value of May–October rainfall for 1951–2013. Unit is in mm/day.

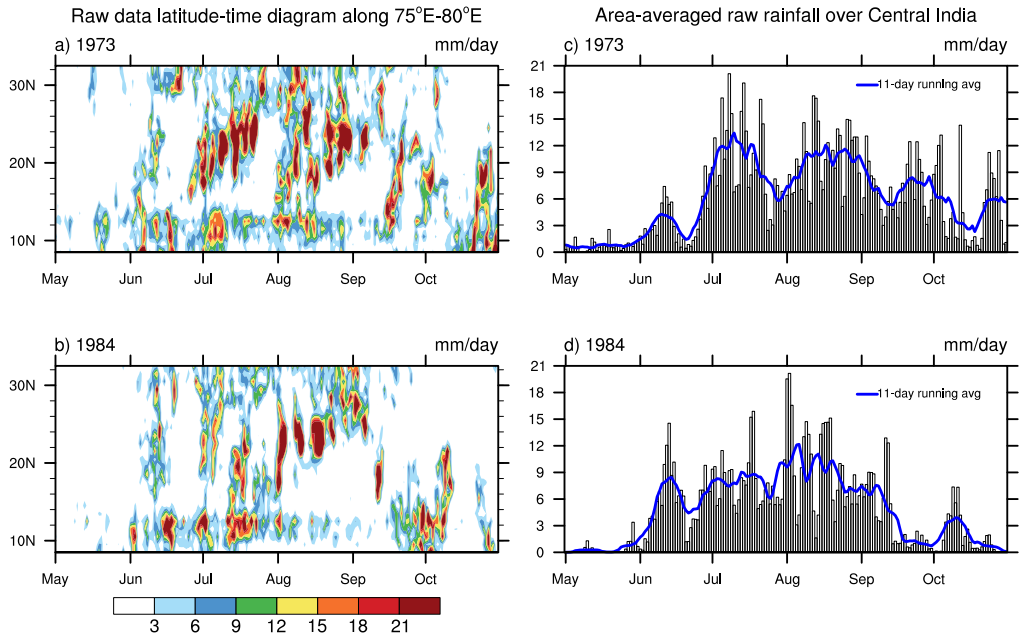

Figure S4: **(a)** Time-latitude diagram of raw rainfall data averaged along 75°E-80°E during 1973 May–October. **(b)** Same as (a), but for 1984. **(c)** Time series of daily rainfall over central Indian region (16.5°N to 26.5°N, 74.5°E to 86.5°E) for 1973 May–October. Blue line indicates 11-day running average. **(d)** Same as (c), but for 1984.

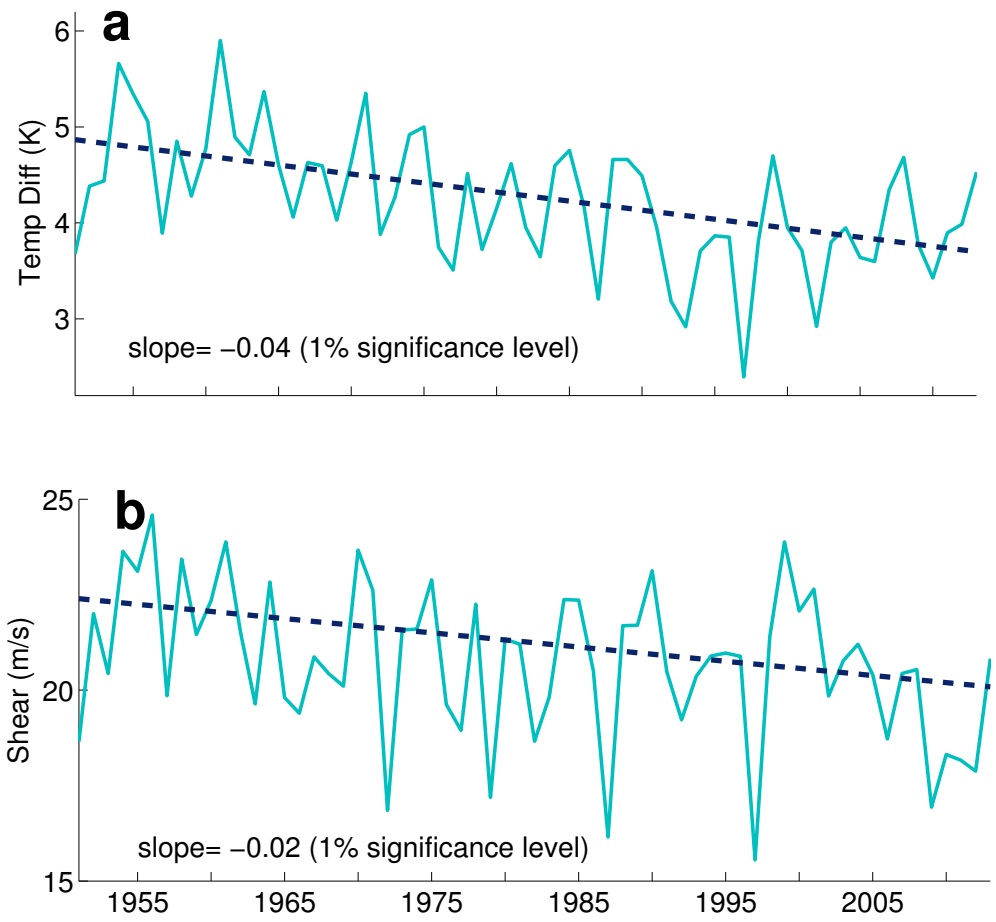

Figure S5: **(a)** Upper tropospheric (200hPa) meridional temperature gradient in May–October during 1951–2013 calculated as the difference between 200hPa temperature averaged over Tibetan region ($30°N$–$35°N$, $80°E$–$90°E$) and equatorial Indian ocean ($5°S$–$5°N$, $70°E$–$90°E$). **(b)** Absolute value of vertical shear of zonal winds ($U_{200hPa} - U_{850hPa}$) over Indian monsoon region ($5°N$–$20°N$, $70°E$–$85°E$). Trends are evaluated using Theil-Sen estimator and Mann-Kendall test is used to determine the significance of the trends as in figure 1 in main text. We have used the winds and air temperature dataset for 63 years (1951–2013) from the National Centers for Environmental Prediction–National Center for Atmospheric Research (NCEP–NCAR) reanalysis [8].

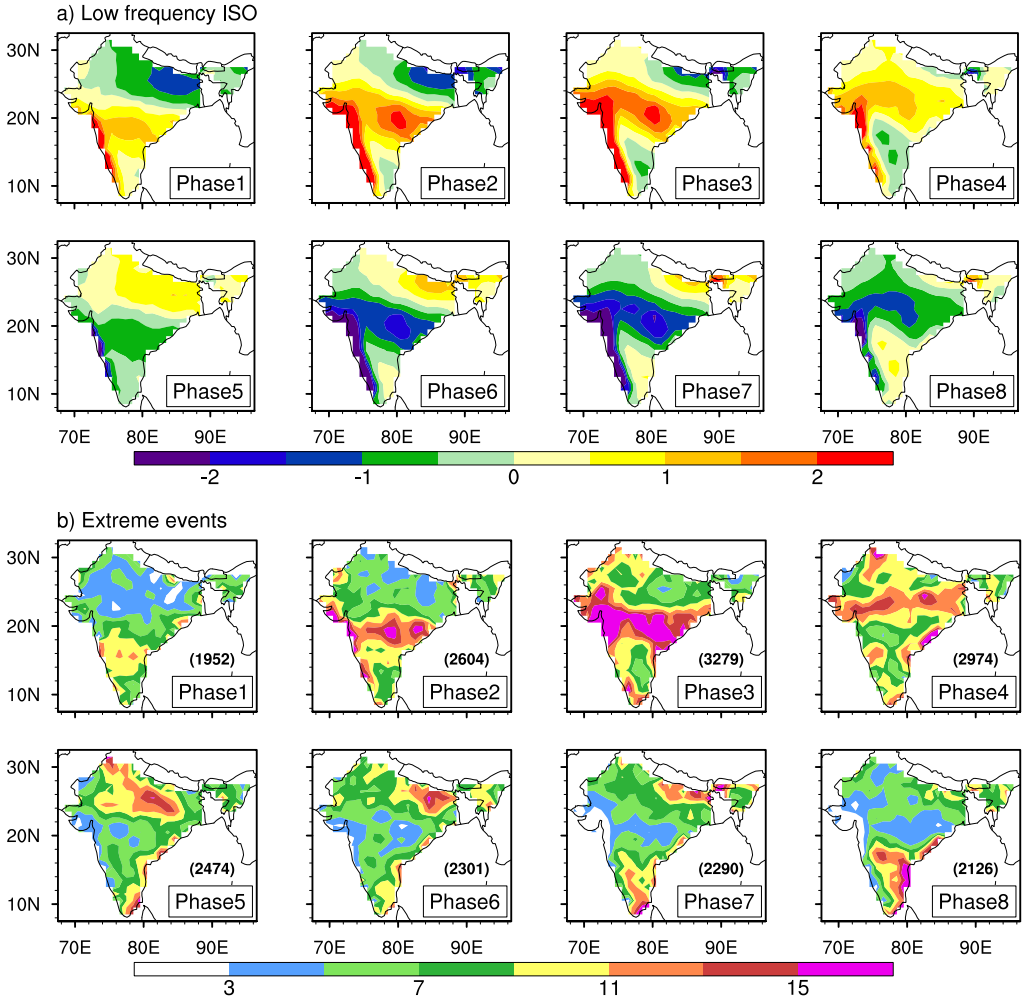

Figure S6: **(a)** Average phase composite structure of LF-ISO during May–October, 1951–2013, calculated as the mean in each phase of the phase composites of all the significant LF-ISO modes found in May–October, 1951–2013, having periodicity within 20–60 days. Unit is in mm/day. and **(b)** Sum of extreme rainfall events occurred in each phase of LF-ISO over the same period in May–October. Numbers in the braces indicate the total extreme events occurred in that particular phase over India in May–October, 1951–2013, indicating most extreme events occur in phase 3 of LF-ISO.

References

[1] Vautard R, Yiou P and Ghil M 1989 Singular-spectrum analysis: A toolkit for short, noisy chaotic signals *Physica* D **58** 95–126 (doi: 10.1016/0167-2789(92)90103-T).

[2] Ghil M *et al* 2002 Advanced spectral methods for climatic time series *Rev. Geophys.* **40** 1003 (doi:10.1029/2000RG000092).

[3] Plaut G and Vautard R 1994 Spells of low-frequency oscillations and weather regimes in the Northern Hemisphere *J. Atmos. Sci.* **51** 210–236 (doi:10.1175/1520-0469(1994)051).

[4] Allen M R and Robertson A W 1996 Distinguishing modulated oscillations from coloured noise in multivariate data sets *Clim. Dyn.* **12** 775–784 (doi:10.1007/s003820050142).

[5] Moron V, Vautard R and Ghil M 1998 Trends, interdecadal and interannual oscillations in global sea-surface temperatures *Clim. Dyn.* **14** 545–569 (doi:10.1007/s003820050241).

[6] Groth A and Ghil M 2011 Multivariate singular spectrum analysis and the road to phase synchronization *Phys. Rev.* **84E** 036206 (doi: 10.1103/PhysRevE.84.036206).

[7] Helsel D R and Hirsch R M 1992 *Statistical Methods in Water Resources* (Elsevier Science).

[8] Kalnay E *et al* 1996 The NCEP/NCAR 40-Year Reanalysis Project *Bull. Amer. Meteor. Soc.* **77** 437–471.